Marine Pollution Bulletin 140 (2019) 509–522

Contents lists available at ScienceDirect

Marine Pollution Bulletin

journal homepage: www.elsevier.com/locate/marpolbul

Soundscape of an Indo-Pacific humpback dolphin (*Sousa chinensis*) hotspot before windfarm construction in the Pearl River Estuary, China: Do dolphin engage in noise avoidance and passive eavesdropping behavior?

Zhi-Tao Wang[a], Tomonari Akamatsu[b], Douglas P. Nowacek[c,d], Jing Yuan[a,e], Lu Zhou[a,e], Pei-Yu Lei[a,e], Jiao Li[a,e], Peng-Xiang Duan[a], Ke-Xiong Wang[a,*], Ding Wang[a,*]

[a] The Key Laboratory of Aquatic Biodiversity and Conservation of the Chinese Academy of Sciences, Institute of Hydrobiology of the Chinese Academy of Sciences, Wuhan 430072, PR China
[b] National Research Institute of Fisheries Science, Fisheries Research and Development Agency, Fukuura, Kanagawa 236-8648, Japan
[c] Nicholas School of the Environment, Duke University Marine Laboratory, Beaufort, NC 28516, USA
[d] Pratt School of Engineering, Duke University, Durham, NC 27708, USA
[e] University of Chinese Academy of Sciences, Beijing 100039, PR China

ARTICLE INFO

Keywords:
Soundscape
Acoustics
Chinese white dolphin
Dolphin vocalization
Fish vocalization
Windfarm

ABSTRACT

Soundscapes are vital to acoustically specialized animals. Using passive acoustic monitoring data, the temporal and spectral variations in the soundscape of a Chinese white dolphin hotspot were analyzed. By cluster analysis, the 1/3 octave band power spectrum can be grouped into three bands with median overall contribution rates of 35.24, 14.14 and 30.61%. Significant diel and tidal soundscape variations were observed with a generalized linear model. Temporal patterns and frequency ranges of middle frequency band sound matched well with those of fish vocalization, indicating that fish might serve as a signal source. Dolphin sounds were mainly detected in periods involving low levels of ambient sound and without fish vocalization, which could reflect noise avoidance and passive eavesdropping behaviors engaged in by the predator. Pre-construction data can be used to assess the effects of offshore windfarms on acoustic environments and aquatic animals by comparing them with the soundscape of postconstruction and/or postmitigation.

1. Introduction

Soundscape ecology, defined as the study of the acoustic characteristics of any acoustic environment, aims to discern the contributions of human and nonhuman activity-related sound sources (Pijanowski et al., 2011a, 2011b; Staaterman et al., 2013, 2014). Soundscapes are typically composed of three fundamental elements: anthrophony (sound generated through human activities such as outboard engine noise or sonar pings), biophony (sound generated by aquatic animals, including vocal and nonvocal activities such as sounds of mollusks feeding) (Kitting, 1979) and geophony (sound generated through physical features such as seismological activity, waves and rain) (Pijanowski et al., 2011a, 2011b; Montgomery and Radford, 2017). The acoustic characteristics of marine habitats are increasingly being considered as key environmental variables and particularly for acoustically specialized fauna such as dolphins.

Many marine organisms, including invertebrates, fish and marine mammals, whales and dolphins in particular, use acoustic cues to facilitate the accomplishment of some vital life functions such as communication, navigation, foraging, reproduction and predator avoidance (Simpson et al., 2016; Haver et al., 2018). Ocean soundscapes also carry important dynamic and sensory information in space and time on habitat quality (Coquereau et al., 2017), and fish and crustacean larvae seem to use acoustic cues for spatial orientations, may be able to discriminate between habitats with distinct underwater sound signatures (Radford et al., 2010) and select suitable ambient sound habitat for settlement (Slabbekoorn and Bouton, 2008). Human activities coupled with global climate change are currently accelerating changes occurring in estuarine–coastal ecosystems at an unprecedented rate (Cloern et al., 2016). Human activity-generated anthrophonic sounds may mask biophonic sounds and may impede an animal's ability to perform the abovementioned vital survival functions.

Anthropogenic ocean noise has magnified over the last few decade (Hildebrand, 2009; Ellison et al., 2012) and some noise sources such as

* Corresponding authors.
E-mail addresses: wangk@ihb.ac.cn (K.-X. Wang), wangd@ihb.ac.cn (D. Wang).

https://doi.org/10.1016/j.marpolbul.2019.02.013
Received 22 December 2018; Received in revised form 6 February 2019; Accepted 6 February 2019
Available online 11 February 2019
0025-326X/

shipping and seismic airgun surveys have been treated as environmental-level stressors (Hildebrand, 2009). Moreover, there has been increasing recognition of and concern for the potentially chronic effects of increases in human activity on marine animals (Ellison et al., 2012). The study of the marine soundscape represents a field of growing interest because of the potential implications it has for the assessment of human–underwater acoustic environment interactions.

The conservation status of Indo-Pacific humpback dolphins (*Sousa chinensis*) meets the International Union for Conservation of Nature's (IUCN's) Red List criteria for classification as Vulnerable (Jefferson and Smith, 2016). This may partially be due to their general preference for estuarine and coastal and shallow water habitats (< 30 m depth), rendering them susceptible to impacts of human activity (Jefferson and Smith, 2016). The conservation management of the majority of the humpback dolphin distribution range is severely inadequate. The world's largest known population of humpback dolphins, with a population size estimated at 2637 (Coefficient of variation of 19% to 89%), is distributed in the Pearl River Estuary (Preen, 2004; Chen et al., 2010; Jefferson and Smith, 2016). However, this population is suffering an annual declining rate of 2.5% (Karczmarski et al., 2016). Beside threats from coastal development, habitat degradation and loss, prey depletion, entanglement in fishing gear and pollutant accumulation, noise pollution is increasingly being considered a key environmental stressor for this species (Karczmarski et al., 2016).

Rapid local development such as through the construction of the Hong Kong-Zhuhai-Macao bridge (Wang et al., 2014b) and the Shenzhen-Zhongshan bridge has already accelerated human damage to coastal ecosystems. In addition, growing demand for environmentally friendly energy has led to an increase in the construction of offshore windfarms and the Guishan windmill farm was authorized to be constructed within the Linding waters of the Pearl River Estuary. Several studies have addressed impacts of the construction and operation of windfarms on marine life and particularly on marine mammals (Madsen et al., 2006; Bailey et al., 2010; Thompson et al., 2010; Dähne et al., 2014). Construction involves many types of activities such as pile driving, which can generate intense sound likely to disrupt the behaviors of marine mammals over several kilometers and to cause hearing impairment within a close range (Madsen et al., 2006). Taking the bottlenose dolphins (*Tursiops truncatus*) in the Moray Firth of NE Scotland as an example, behavioral disturbance can have occur up to 50 km away from a pile driving site and auditory injury occurs within 100 m (Bailey et al., 2010).

The Pearl River Estuary, a hotspot for the humpback dolphins according to on our long-term field survey, has suffered by extraordinarily heavy levels of anthropogenic noise disturbance (Wang et al., 2015b). Despite the use of this area by such an acoustically specialized species, to our knowledge no study has examined any section of the Pearl River Estuary in terms of acoustic components.

Concerns regarding the conservation of the local humpback dolphin population and the management of human activities to mitigate threats are mounting. For instance, the existing baseline soundscape must be measured to protect animals and to understand the threats that they are exposed to (Haver et al., 2018). Thus, this study has the specific objective of identifying: (1) how the soundscape changes over time; (2) the correlation between different frequency bands within the soundscape and their potential relation to environmental factors such as tidal conditions and the time of a day; and (3) prominent sound sources (anthrophonic, biophonic or geophonic), their contributions to the soundscape and their respective frequency bands. The results of this paper also provide a baseline description of the soundscape before the construction of the windfarm and can be used to compare modifications that future windfarm construction and operation may cause while also informing future noise management and mitigation decisions and strategies.

2. Methods

2.1. Acoustic data recording system

Underwater acoustic recordings, including ambient noise and humpback dolphin whistles, were created using a Song Meter Marine Recorder (Wildlife Acoustics, Inc., Maynard, MA, USA), which includes a programmable autonomous signal processing unit integrated with a bandpass filter and a pre-amplifier. The recorder can log data at a resolution of 16 bits and at a 96 kHz sampling rate, with a storage capacity of 512 GB and includes an HTI piezoelectric omnidirectional hydrophone (model HTI-96-MIN; High Tech, Inc., Long Beach, MS, USA; sensitivity: −164 dB re 1 V/μPa at 1 m distance; recording bandwidth: 2 Hz–48 kHz; flat frequency response: 2 Hz–37 kHz (± 3 dB)). The signal processing unit was sealed within a water proof PVC housing and was submersible to 150 m. The recording system was calibrated prior to shipment from the manufacturer.

Another self-contained and submersible acoustic data logger, A-tag (ML200-AS2, Marine Micro Technology, Saitama, Japan) (Akamatsu et al., 2005), was used to monitor the high frequency biosonar sounds of humpback dolphins (Wang et al., 2015b).

2.2. Data collection

Stationary underwater acoustic monitoring was conducted at the underwater base of a passive signal receiving tower (22°07′54″ N, 113°43′54″ E) located between the Sanjiao, Chitan and Datou islands (Fig. 1). The acoustic recording systems (both of the SM2M and A-tag) were attached to a steel wire rope and fixed at 4.0 m above the ocean floor. Depending on tide conditions, the recorder was positioned approximately 3.0 to 5.8 m below the water surface. The steel wire rope was suspended below the signal tower and a 40 kg anchor block was attached to the bottom of the steel wire rope to limit the movement of the recording system due to water currents (Fig. 1). SM2M recordings were taken continuously at a 96 kHz sampling rate during deployment periods running from May 26 to June 4, 2014 and from June 17 to 22, 2014.

2.3. Acoustic data analysis

Upon the retrieval of the recorder, acoustic data were downloaded and processed. For the noise analysis, a custom developed acoustic analysis routine through MATLAB 7.11.0 (The Mathworks, Natick, MA, USA) was used. Parameters of the sound pressure levels (SPLs) and 1/3 octave band frequency spectrum were continuously analyzed each second. SPLs were directly derived from pressure metrics, including zero-to-peak sound pressure (SP_{pk}) and root-mean-square sound pressure (SP_{rms}) values. SP_{pk} was measured as the maximum of the unweighted absolute instantaneous sound pressure in the measurement bandwidth and SP_{rms} was measured as the average of the square of unweighted instantaneous sound pressure in the measurement bandwidth integrated over the analyzed signal duration. SPL_{pk} and SPL_{rms} are ten times the logarithm to base 10 of the ratio of the square of SP_{pk} and SP_{rms}, respectively, to the square of the reference sound pressure of 1 μPa. Power spectral density (PSD) level routines (dB re 1 $\mu Pa^2\ Hz^{-1}$) were applied to investigate the narrowband power spectra in each 1 Hz band using the Welch approach (Wang et al., 2016). All SPL and PSD levels were adjusted according to overall system sensitivity values (hydrophone sensitivity and preamplifier gain) to determine absolute results.

Since 1/3 of an octave band approximates the effective filter bandwidth of cetaceans (Richardson et al., 1995), the 1/3 octave band frequency spectrum was investigated by summing the power of all 1 Hz bands within each 1/3 octave to assess potential impacts of noise on mammalian hearing. The frequency boundaries of each 1/3 octave band were determined according to the ANSI S 1.6-1986 and ISO

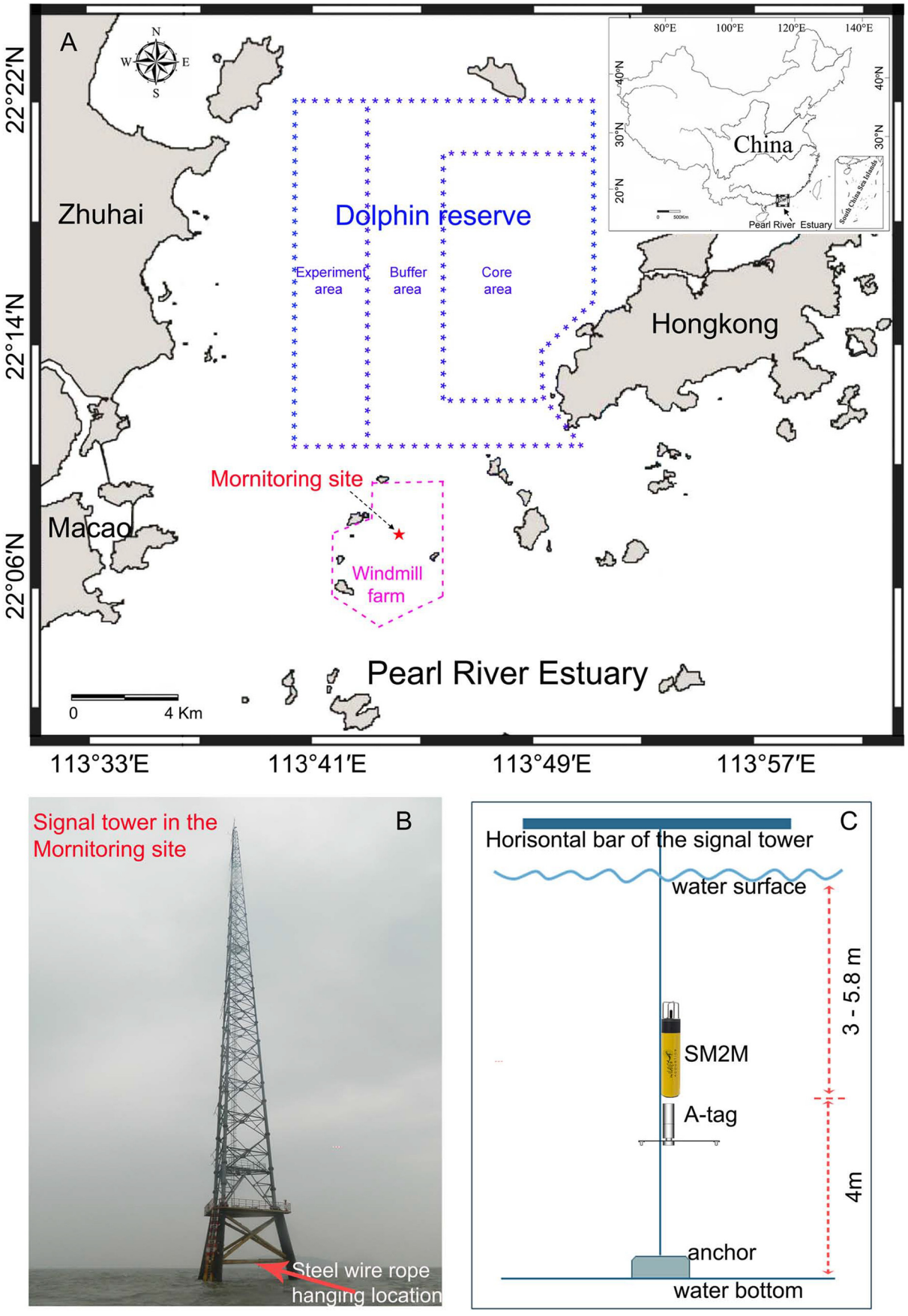

Fig. 1. Map of the static acoustic monitoring area (A) and schematic of the equipment deployment (B and C). Monitoring devices (including SM2M and A-tag) were suspended below the signal tower.

266:1997(E) and were designated by each preferred center frequency (Table S1). In accordance with the recording bandwidth of the recorder, we only investigate a frequency range of 2.82–44,686 Hz, which covers 42 1/3 octave bands and with a corresponding center frequency of 3.15 Hz–40 kHz (Table S1). To enhance the calculation performance of PC, SPL_{rms} and PSD were further averaged to determine the mean results for each min. at the intensity of the signal before converting to dB.

2.4. Similarity and cluster analysis of the 1/3 octave band power spectrum

The correlation between the 42 1/3 octave band power spectrum was investigated by Spearman's rank order correlation (Romesburg, 2004). A hierarchical cluster analysis (Romesburg, 2004), a step wise process that merges the two closest or furthest data points at each step and that builds a hierarchy of clusters based on distances between them, was applied to identify similar 1/3 octave band power spectra.

The 24 h of the day were divided into five consecutive diel phases in sequences of night1, morning, day, evening and night2 phases (the specific partitioning method used is described in the following publications) (Todd et al., 2009; Wang et al., 2014a, 2015b). The tidal period for the Pearl-River Estuary is semidiurnal (12 + hour) and tidal conditions were divided into four consecutive phases: low, flood, high, and ebb (the specific partitioning method used is described in the following publications) (Guilherme-Silveira and Silva, 2009; Fury and Harrison, 2011; Wang et al., 2015b). Time points used for the separation of different tidal phases were obtained from the China Shipping Service (CNSS) website (http://ocean.cnss.com.cn/).

2.5. Statistical analysis

Descriptive statistics were used to summarize the acoustic parameters. All parameters were tested for normality and homoscedasticity with a Kolmogorov–Smirnov test (for data sets ≥ 50) and Levene's test for equality of variance, respectively (Zar, 1999). Because of the grossly skewed distribution of the majority of the data, descriptive parameters for the median, quartile deviation (QD), 5th percentile (P5), and 95th percentile (P95) were adopted. For the analysis of the difference in the broadband SPL_{rms} and the subdivided three frequency band SPLs as a function of diel and tidal conditions, a generalized linear model (GLM) analysis of variance (ANOVA) was applied with a two-way ANOVA (diel x tidal) full factorial design by including diel and tidal data into the model as main factors and by building interaction terms into the model. When significant differences were found for either main factor, more focused analyses of the post-hoc pair wise multiple comparison tests were performed using either Tukey's HSD method (when Levene's test for equality of variance indicated no homogeneous variances, $p > 0.05$) or Tamhane's T2 method (when equal variances could not be assumed, $p < 0.05$) to determine which levels of each factor significantly differed. Statistical analyses were performed using SPSS 16.0 for Windows (SPSS Inc., Chicago, IL, USA). Probability values exceeding 0.05 were considered to denote a critical statistical level of significance.

2.6. Fish and humpback dolphin sound analysis

Humpback dolphin whistles were frequency modulated tonal signals characterized by a mean duration of 370 ms (range: 22–2923 ms) and a fundamental contour range from 250 Hz to 33,000 Hz and exhibiting a harmonic structure (Fig. 2, see Wang et al. (2013) for a detailed demonstration of a spectrogram). Fish sounds in the Pearl River Estuary tend to include a pulse train structure with a peak frequency of 500 to 2600 Hz and with majority of energy falling below 4000 Hz (Fig. 2, see Wang et al. (2017) for a detailed demonstration of a spectrogram). For fish sound and humpback dolphin whistle analysis, SM2M data were inspected with a spectrogram visually and aurally using RAVEN PRO Bioacoustics software (version 1.4; Cornell Laboratory of Ornithology, Ithaca, NY). The parameter settings used were as follows: the Hanning window function, a temporal grid spacing of 4.27 ms with an overlap of 80%, and a frequency grid resolution of 46.9 Hz with a window size and fast Fourier transform (FFT) size of 2048. Fish sound counting was based on bouts of pulses.

For the humpback dolphin echolocation click analysis, A-tag data were analyzed using a custom-made multiparameter filter program developed with Igor Pro 5.01 software (Wave Metrics, Lake Oswego, OR, USA) (Wang et al., 2015a, 2015b). Humpback dolphin echolocation click counts were based on bouts of click trains consisting of > 5 clicks (Wang et al., 2015b).

3. Results

3.1. Fish sound detection

A snapshot of dynamic patterns of the soundscape in the Pearl River Estuary can be observed in Fig. 3. The signal source of noise in the frequency band of 10 to 100 Hz, accounting for the loudest energy during the 48-h period remains unknown but may involve shipping activity.

Fish sounds were observed daily during the recording period. Groups of animals occasionally called at the same time over multiple hours and especially before dusk through a phenomenon known as fish chorus (Fig. 3). Fish sound detection rates were also analyzed with results expressed as the number of fish sounds detected per min (Fig. 4B). The majority of the fish acoustics were detected from dusk until dawn of the following day (Fig. 4B).

3.2. Humpback dolphin sound detection

Humpback dolphin whistles and clicks were used as indicators of dolphin presence in the vicinity of the recorder. During the monitoring period, humpback dolphin whistles were detected every day and a total of 851 whistles were detected (Fig. 4A). Humpback dolphin click trains were also detected during most of the monitoring periods and 140 humpback dolphin click trains were detected in total (Fig. 4A). Most humpback dolphin sounds were observed during the day (Fig. 4A).

3.3. SPL_{rms}, SPL_{pk} and 1/3 octave band power spectrum

The broad band SPL_{rms} of the PRE was measured as 121.05 ± 8.44 dB (median ± QD) with a P5-P95 range of 113.44–141.62 dB (Fig. 5A). The SPL_{pk} value for each minute of the Pearl River Estuary was measured as 162.25 ± 1.94 dB (median ± QD), with a P5-P95 range of 157.59–163.99 dB (Fig. 5B).

Dynamic patterns of each 1/3 octave band power spectrum of the Pear River Estuary are shown in Figs. 6 and 7. Three types of spectra can be identified in all 1/3 octave band power spectra, with representative power spectral bands of 20 Hz, 2.5 kHz and 16 kHz (Fig. 7). One third octave band power spectrum of the 20 Hz and 2.5 kHz bands is characterized by three and one peak time each day, respectively (Fig. 6). Fluctuations of the 1/3 octave band power spectrum of 16 kHz are minor with no obvious peak time observed (Fig. 6).

3.4. Similarity and cluster analysis of the 1/3 octave band power spectrum

Euclidean distances among the 42 1/3 octave band sound pressure levels and an additional cluster analysis are shown in Fig. 8 and three clusters can be identified from all 1/3 octave band power spectra, with the low frequency band, middle frequency band and high frequency band covering frequency ranges of 2.82–281 Hz, 282–2238 and 2239–44,686 Hz, respectively. Corresponding center frequencies are valued at 3.16–250, 315–2000, and 2500–40,000 Hz, respectively (Table S2).

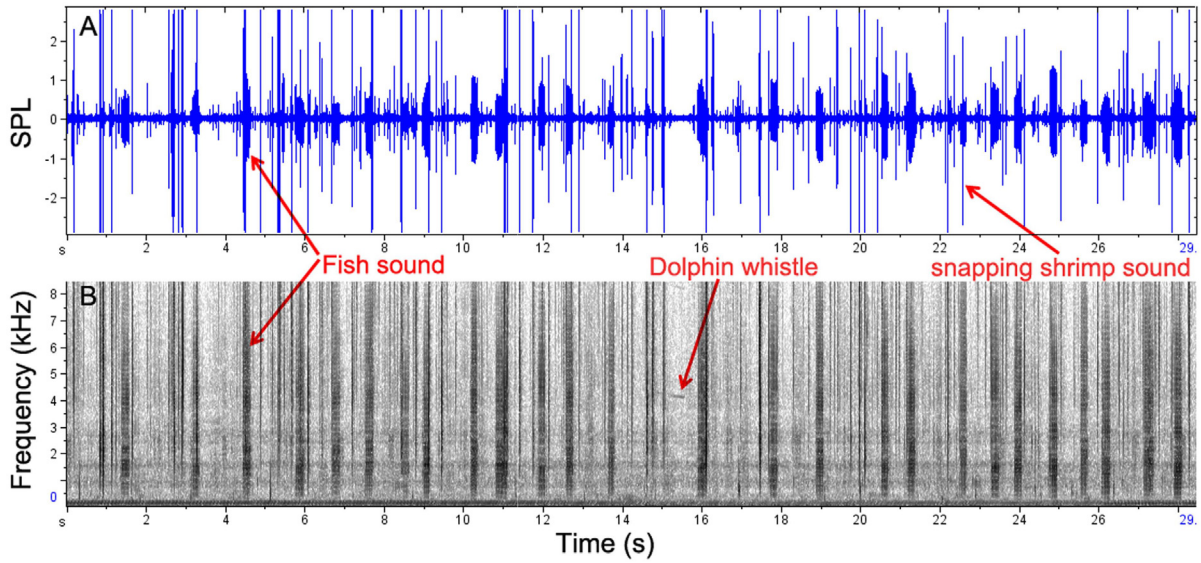

Fig. 2. Waveform (A) and spectrogram (B) of a signal slice illustrating dolphin whistle, fish sound and snapping shrimp sound. Humpback dolphin whistles were frequency modulated tonal signal. Fish sounds tend to include a pulse train structure and with majority of energy falling below 4000 Hz. Snapping shrimp can produce very broad band impulsive signal. The spectrogram parameter settings were Hanning window function, a temporal grid spacing of 4.27 ms with an overlap of 80%, and a frequency grid resolution of 46.9 Hz with a window size and fast Fourier transform (FFT) size of 2048. Note that the spectrogram maximum frequency was scaled to 8.5 kHz for a detailed view of the whistle fundamental frequency.

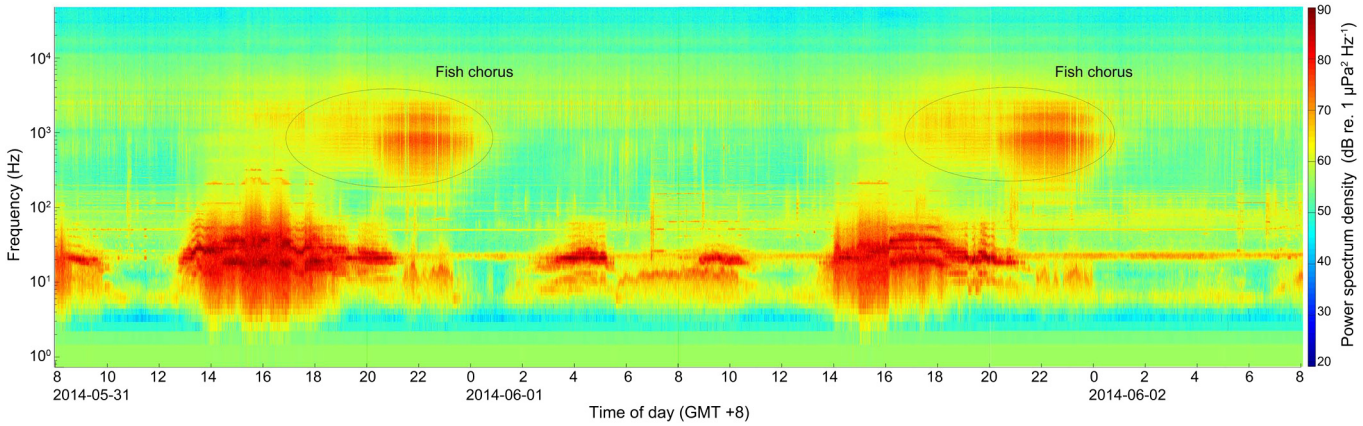

Fig. 3. Spectrogram showing the frequency distribution (Y axis) of sound energy over time (X axis) for 48 h of the soundscape of the Pearl River Estuary. For a better view of the low frequency band, the frequency axis (Y axis) is given in log scale.

3.5. Temporal patterns of SPL_{lfb}, SPL_{mfb} and SPL_{hfb} and their contributions

Temporal patterns of the broadband SPL of the low frequency band (SPL_{lfb}), middle frequency band (SPL_{mfb}) and high frequency band (SPL_{hfb}) are shown in Fig. 9. The SPL_{lfb} is valued at 114.17 ± 12.58 dB (median ± QD) with a P5-P95 range of 100.27–141.59 dB (bar plot in Fig. 9A). The SPL_{mfb} is valued at 111.85 ± 3.41 dB (median ± QD) with a P5-P95 range of 104.76–124.61 dB (bar plot in Fig. 9B). The SPL_{hfb} is valued at 115 ± 1.48 dB (median ± QD) with a P5-P95 range of 111.18–119.73 dB (bar plot in Fig. 9C).

Contributions of the three band SPL (SPL_{lfb}, SPL_{mfb} and SPL_{hfb}) to the overall ambient SPL varied with time (Fig. 10). Relative to the peak contribution time of the low frequency band (Fig. 10B), the peak contribution time of the middle frequency band (Fig. 10C) and low frequency band (Fig. 10D) lagged behind. This phenomenon is also observed in the aligned line plot of the sound pressure level of the three frequency bands (Fig. S1). Contribution rate of lower than 10% of the overall ambient SPL by SPL_{lfb}, SPL_{mfb} and SPL_{hfb} are valued at 25.3%, 42.3% and 39.9%, respectively, for the recording period. Contribution rates exceeding 90% of the overall ambient SPL by SPL_{lfb} and SPL_{mfb} are valued at 32.3% and 2.9%, respectively, for the recording period (Fig. 10E). Contribution rates of higher than 80% of the overall ambient SPL by SPL_{hfb} are valued at 0.9% with a maximum contribution rate of 87.88% (Fig. 10E). Contribution rates to the overall ambient SPL for SPL_{lfb}, SPL_{mfb} and SPL_{hfb} are valued at 35.24 ± 43.11, 14.14 ± 12.36 and 30.61 ± 29.31(median ± QD) percent, respectively, with P5-P95 ranges of 1.31–99.53, 0.17–64.78 and 0.26–74.01%, respectively (Fig. 10F).

3.6. Correlation between the SPL and dolphin and fish sound detection rates

The temporal pattern of the fish sound detection rate closely matches that of SPL_{mfb} (Fig. S2). The majority of humpback dolphin sounds (including whistles and clicks) were detected during periods involving low ambient sound levels (Fig. 11A). Additionally, the majority of humpback dolphin sounds (including whistles and clicks) were detected during periods without fish sounds (Fig. 11B).

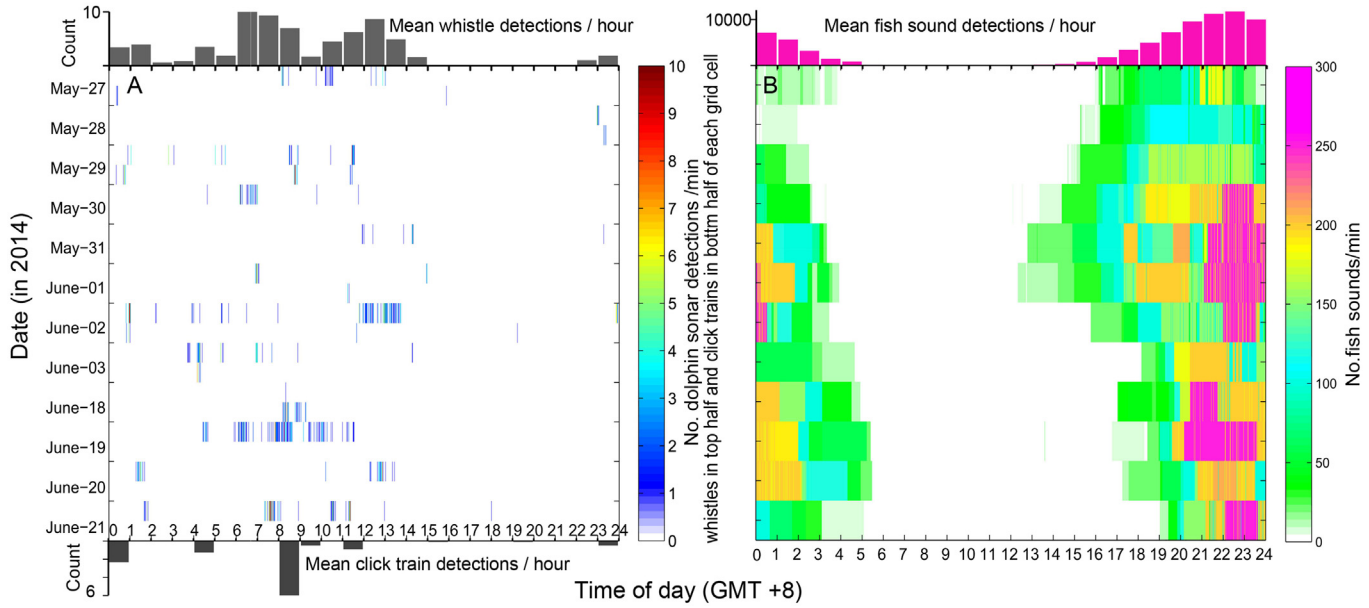

Fig. 4. Sound production rates for humpback dolphins (A) and fish (B) as a function of the time of day (X axis) and date (Y axis). Sound detection rates per min are indicated by colors. Dolphin whistles are denoted in the top half of each grid cell and dolphin click train detection is denoted along the bottom half of each grid cell in A. The averaged No. of dolphin whistles (histograms above A), click trains (histograms below A) and fish acoustics (histograms above B) per hour is also given as a bar plot.

3.7. Cluster and similarity analyse of SPL_{rms}, SPL_{lfb}, SPL_{mfb} and SPL_{hfb}

Cluster and similarity analyse of broadband SPL_{rms} and SPL of the subdivided three frequency bands (SPL_{lfb}, SPL_{mfb} and SPL_{hfb}) are show in Fig. S3. SPL_{lfb} and SPL_{rms} are clustered into one clade while SPL_{mfb} and SPL_{hfb} are grouped into another clade (Fig. S3).

3.8. Diel patterns of SPL_{rms}, SPL_{lfb}, SPL_{mfb} and SPL_{hfb}

The results of the GLM ANOVA indicate that significant differences in diel patterns exist between the SPL_{rms} and all the subdivided SPL_{lfb}, SPL_{mfb} and SPL_{hfb} values (Table 1).

In particular, evening SPL_{rms} values (median ± QD: 132.32 ± 8.81) are significantly higher than night2 (median ± QD: 127.80 ± 7.94), daytime (median ± QD: 119.88 ± 9.77), night1 (median ± QD: 116.64 ± 3.65) and morning values (median ± QD:

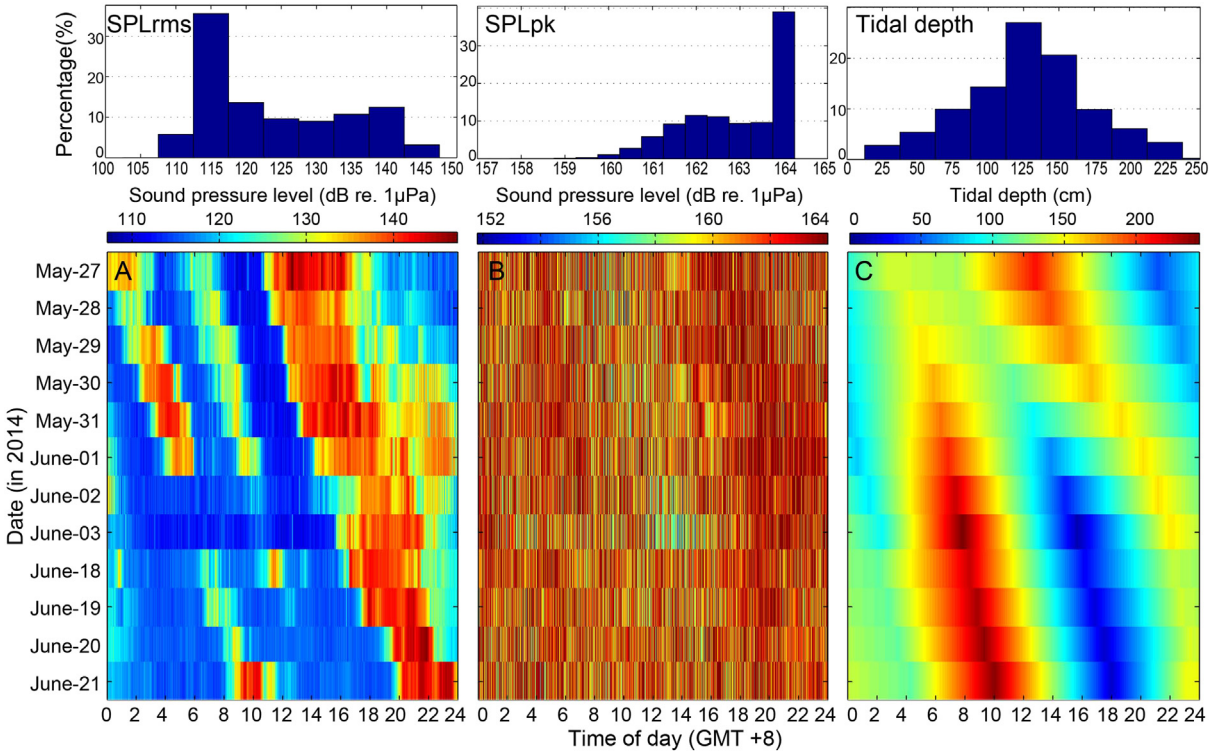

Fig. 5. (A)Root-mean-square, (B) zero-to-peak SPL and (C) tidal conditions of the Pearl River Estuary as a function of the time of day (X axis) and date (Y axis).

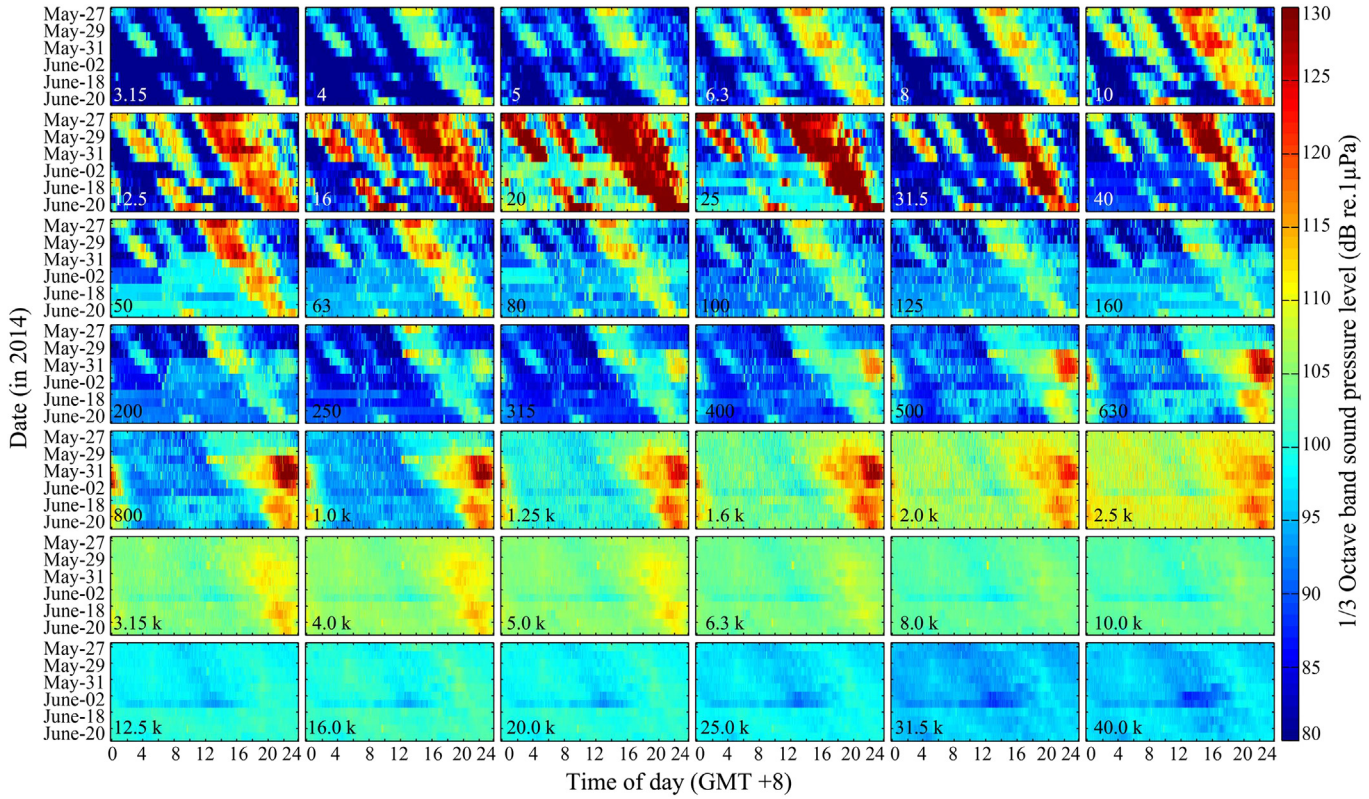

Fig. 6. Temporal patterns of the one third octave band power spectrum (3.15 Hz–40 kHz) of the soundscape as a function of the time of day (X axis) and date (Y axis). Three types of temporal patterns can be identified with representative power spectral bands of 20 Hz, 2.5 kHz and 16 kHz.

115.68 ± 1.60), where significant difference are also observed between each diel phase (Tamhane's T2 post-hoc multiple-comparison test; $p < 0.05$) (Fig. 12A).

SPL_{lfb} for the evening (median ± QD: 132.47 ± 11.08) were significantly higher than that for the daytime (median ± QD: 118.63 ± 13.44), for night2 (median ± QD: 118.31 ± 11.97), for night1 (median ± QD: 108.43 ± 6.25) and for the morning where significant differences are also observed between each diel phase (Tamhane's T2 post-hoc multiple-comparison test; $p < 0.05$) (Fig. 12A).

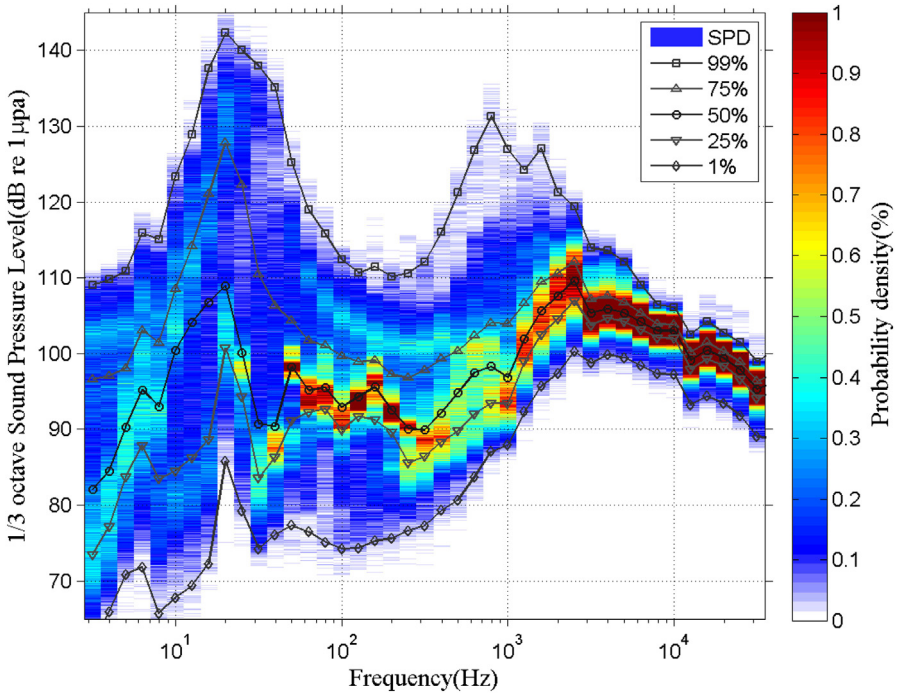

Fig. 7. Spectrum probability density (PSD) of the 42 1/3 octave band sound pressure level for the whole monitoring period. Percentile results of P1, P25, P50, P75 and P99 represent the point for 1%, 25%, 50%, 75% and 99% of the results in an ordered set.

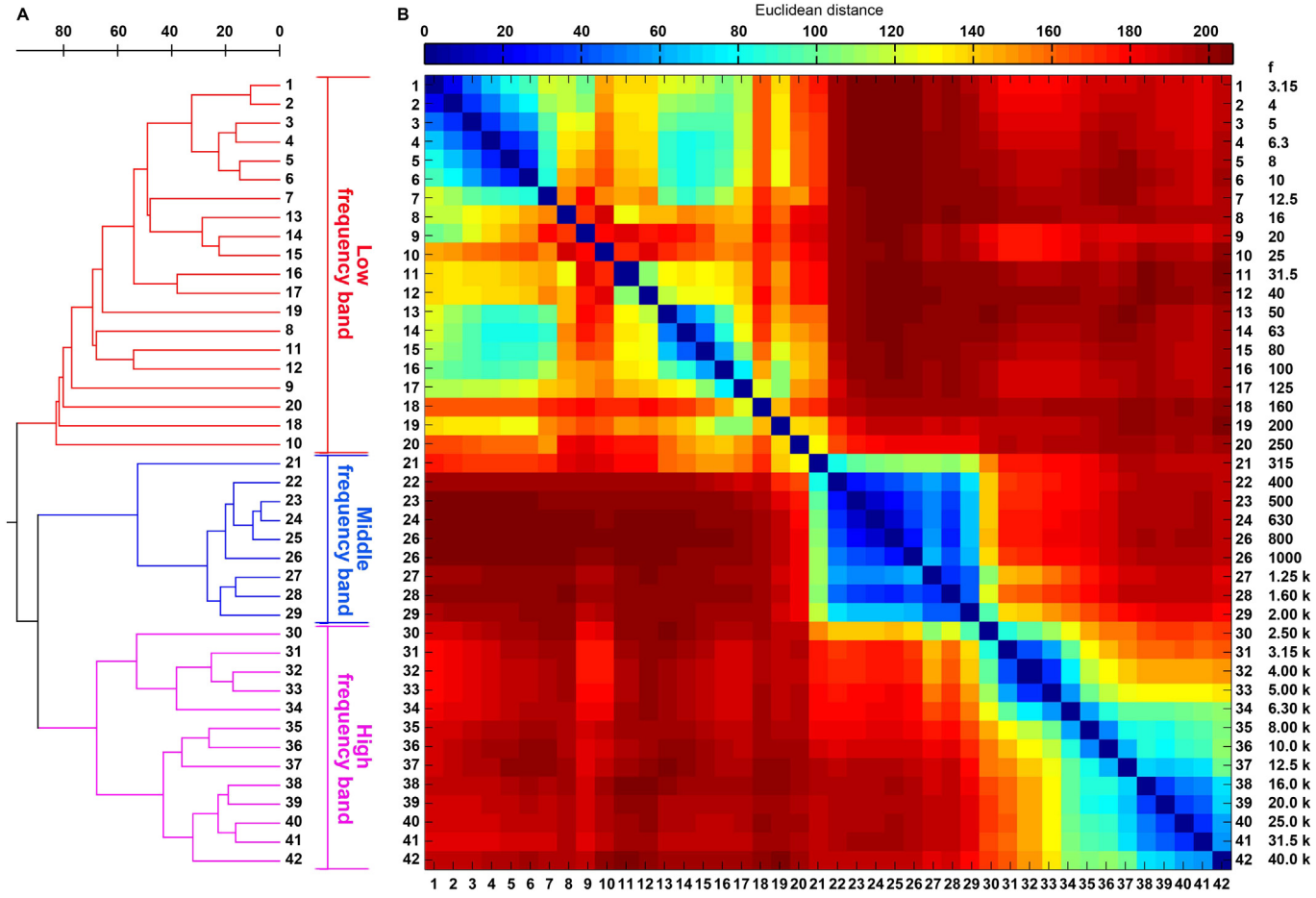

Fig. 8. (A) Cluster analysis and (B) similarity and distance analysis of 42 one third octave band sound pressure levels for the whole monitoring period.

SPL_{mfb} for night2 (median ± QD: 120.10 ± 4.55) is significantly higher than that for the evening (median ± QD: 116.30 ± 3.21), night1 (median ± QD: 110.85 ± 2.61), daytime (median ± QD: 110.62 ± 2.75) and morning (median ± QD: 109.63 ± 2.43) where significant differences were also observed between each diel phase (Tamhane's T2 post-hoc multiple-comparison test; $p < 0.05$) (Fig. 12A).

Significant differences in SPL_{hfb} are observed for night1 (median ± QD: 114.56 ± 1.21), the morning (median ± QD: 114.82 ± 1.16), the daytime (median ± QD: 114.42 ± 1.28), the evening (median ± QD: 117.34 ± 1.19) and night2 (median ± QD: 117.84 ± 1.80) (Tamhane's T2 post-hoc multiple-comparison test; $p < 0.05$) (Fig. 12) except for those between at night1 and the morning and for between the morning and daytime (Tamhane's T2 post-hoc multiple-comparison test; $p > 0.05$) (Fig. 12A).

3.9. SPL_{rms}, SPL_{lfb}, SPL_{mfb} and SPL_{hfb} and tidal conditions

Both dynamic patterns of SPL_{rms} and SPL_{lfb} do not coincide with local tidal conditions (Fig. 13). The peak SPL_{rms} (Fig. 13A) and SPL_{lfb} (Fig. 13B) time points are not in phase with the highest and/or lowest water levels (including the first and second highest water levels and the first and second lowest water levels).

The results of the GLM ANOVA indicate that significant differences exist between all parameters of SPL_{rms} and between subdivided SPL_{lfb}, SPL_{mfb} and SPL_{hfb} values across tidal phases (Table 1). Specifically, SPL_{rms} for ebb tide (median ± QD: 129.51 ± 11.83) is significantly higher than those of the low tide (median ± QD: 126.33 ± 10.08), flood tide (median ± QD: 119.91 ± 6.32), and high tide (median ± QD: 116.45 ± 3.18) where significant differences are also observed between each tidal phase (Tamhane's T2 post-hoc multiple-comparison test; $p < 0.05$) (Fig. 12B). The ebb tide SPL_{lfb} value (median ± QD: 129.96 ± 16.17) is significantly higher than those of the low tide (median ± QD: 124.53 ± 13.59), flood tide (median ± QD: 112.88 ± 8.80), and high tide periods (median ± QD: 108.08 ± 5.58) where significant difference are also observed between each tidal phase (Tamhane's T2 post-hoc multiple-comparison test; $p < 0.05$) (Fig. 12B). The low tide SPL_{mfb} value (median ± QD: 113.07 ± 4.57) is significantly higher than that those of the flood tide (median ± QD: 112.03 ± 3.47), ebb tide (median ± QD: 111.42 ± 3.31) and high tide period (median ± QD: 110.91 ± 3.12), where significant differences are also observed between each tidal phase (Tamhane's T2 post-hoc multiple-comparison test; $p < 0.05$) (Fig. 12B). The low tide SPL_{hfb} value (median ± QD: 115.60 ± 1.69) is significantly higher than those for the flood tide (median ± QD: 115.27 ± 1.61), ebb tide (median ± QD: 114.68 ± 1.37) and high tide(median ± QD: 114.48 ± 1.47) where significant differences are also observed between each tidal phase (Tamhane's T2 post-hoc multiple-comparison test; $p < 0.05$) (Fig. 12B).

4. Discussion

4.1. Acoustically mediated predator-prey interactions

Historical surveys indicate that no other dolphin species are found in the monitoring site and thus dolphin acoustic identification was not required (Jefferson et al., 2002; Wang et al., 2015b). The majority of humpback dolphin sounds (including whistles and clicks) were detected during periods of low ambient sound levels (Fig. 11A), which might reflect noise avoidance behaviors of this species of dolphin. The

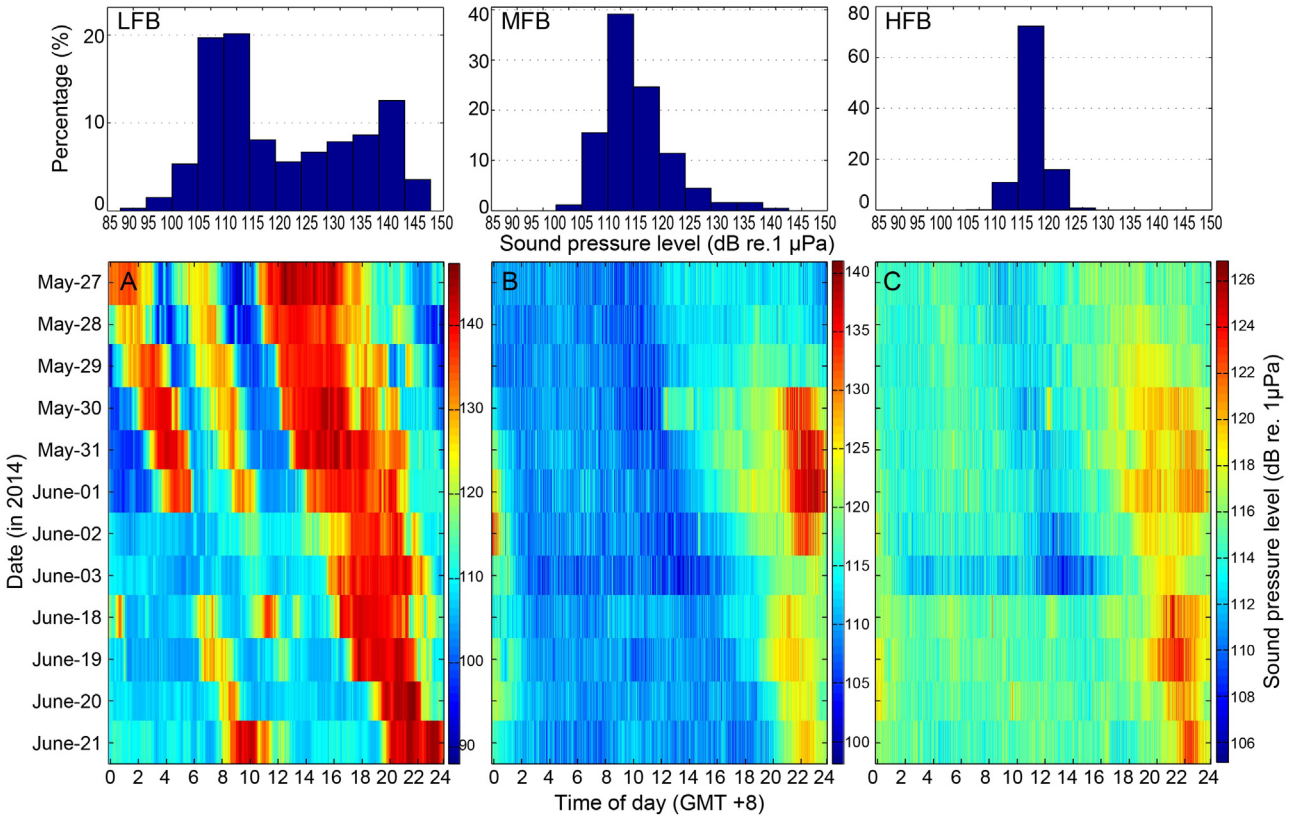

Fig. 9. Sound pressure levels of the three frequency bands (A) low frequency band, (B) middle frequency band and (C) high frequency band as a function of the time of day (X axis) and date (Y axis). Pooled distribution patterns of each band are also given at the top of the maps.

humpback dolphin appears to rely almost exclusively on fish for food (Barros et al., 2004; Parra and Jedensjö, 2014) and the majority of its prey are soniferous fish (Fish and Mowbray, 1970; Banner, 1972; Whitehead and Blaxter, 1989; Ren et al., 2007). In this study, the majority of humpback dolphin sounds (including whistles and clicks) were detected during periods without fish sounds (Fig. 11B). This may be attributable to 'acoustical avoidance' by prey, i.e., adaptive silencing behavior whereby prey stop producing sounds that might give away their location to an acoustically sensitive predator. This type of acoustical avoidance behavior, which might be a common phenomenon in acoustically mediated predator-prey interactions in the sea, has been observed in silver perch (*Bairdiella chrysoura*), which stop chorusing when bottlenose dolphins (*T. truncatus*) vocalize close to spawning aggregations (Luczkovich et al., 2000). As another possible explanation, this phenomenon may serve as an eavesdropping strategy adopted by the predator as observed in bottlenose dolphins, which use passive listening for the purpose of detecting and possibly orienting to their prey (Barros and Myrberg, 1987; Barros, 1993; Gannon et al., 2005). The humpback dolphin whistle (Wang et al., 2013) was distinct from fish sounds in the Pearl River Estuary (Wang et al., 2017) and can be distinguished both spectrally and aurally. While dolphin whistles may have been acoustically masked in periods of high ambient sound pressure levels, rendering dolphin sounds potentially difficult to detect, since we visually and aurally inspected sound spectrograms to detect and confirm the presence of humpback dolphin whistles rather than using an autonomous whistle detector, the percentage of missed dolphin whistles masked by ambient noise or fish chorous can be greatly reduced under very noisy conditions (Fig. 2).

4.2. Acoustic spectrum partition

From this study, via a cluster analysis based on the Euclidean distance between all 1/3 octave band power spectra, three distinct clusters can be objectively identified: the low frequency band, middle frequency band and high frequency band covering frequency ranges of 2.82–281 Hz, 282–2238 and 2239–44,686 Hz, respectively. Wenz (1962) reviewed publications of ocean noise and classified frequencies of below 20,000 Hz into three overlapping spectral components: the 1 Hz–100 Hz band caused by the fluctuations of turbulence and pressure; the 10 Hz–1000 Hz band, which is oceanic traffic related; and the 50 Hz–20,000 Hz band, which is wind dependent and which results from bubbles and spray. Staaterman et al. (2014) also examined the temporal soundscape patterns of a coral reef habitat in the upper Florida Keys and classified the acoustic spectrum into two non-overlapping frequency bands: a low frequency band (25 Hz to 2000 Hz) covering vocalizations and the hearing range of most fish (Tavolga et al., 1981) and a high-frequency band (2000 Hz to 10,000 Hz) covering the frequency range dominated by snapping shrimp (*Alpheus spp.*) and Odontocete vocalization. In Baja California Sur, Mexico, Seger et al. (2015) studied its ambient acoustic environment and defined two bandwidths of biological relevance: a 500 Hz–3120 Hz band dominated by snapping shrimp and a 200 Hz–500 Hz band not including shrimp snapping. The soundscape of a shallow water habitat of a critically endangered Indo-Pacific humpback dolphin off the west coast of Taiwan was also identified by Guan et al. (2015), in which the frequencies were classified into three bands: a 150 Hz–300 Hz band mainly associated with passing container vessels, a 1200 Hz–2400 Hz band ascribed to the sonic fish chorus at nighttime, and a 3000 Hz–6000 Hz band referred to as a dolphin whistle band. However, the above frequency band partitions are more or less subjective. Via cluster analysis, we can group frequency bands in an objective manner.

4.3. Sources origin and contribution of different frequency band

In shallow waters, wind and rain, which can disturb the water's surface, have been proposed as the largest geophonic contributions

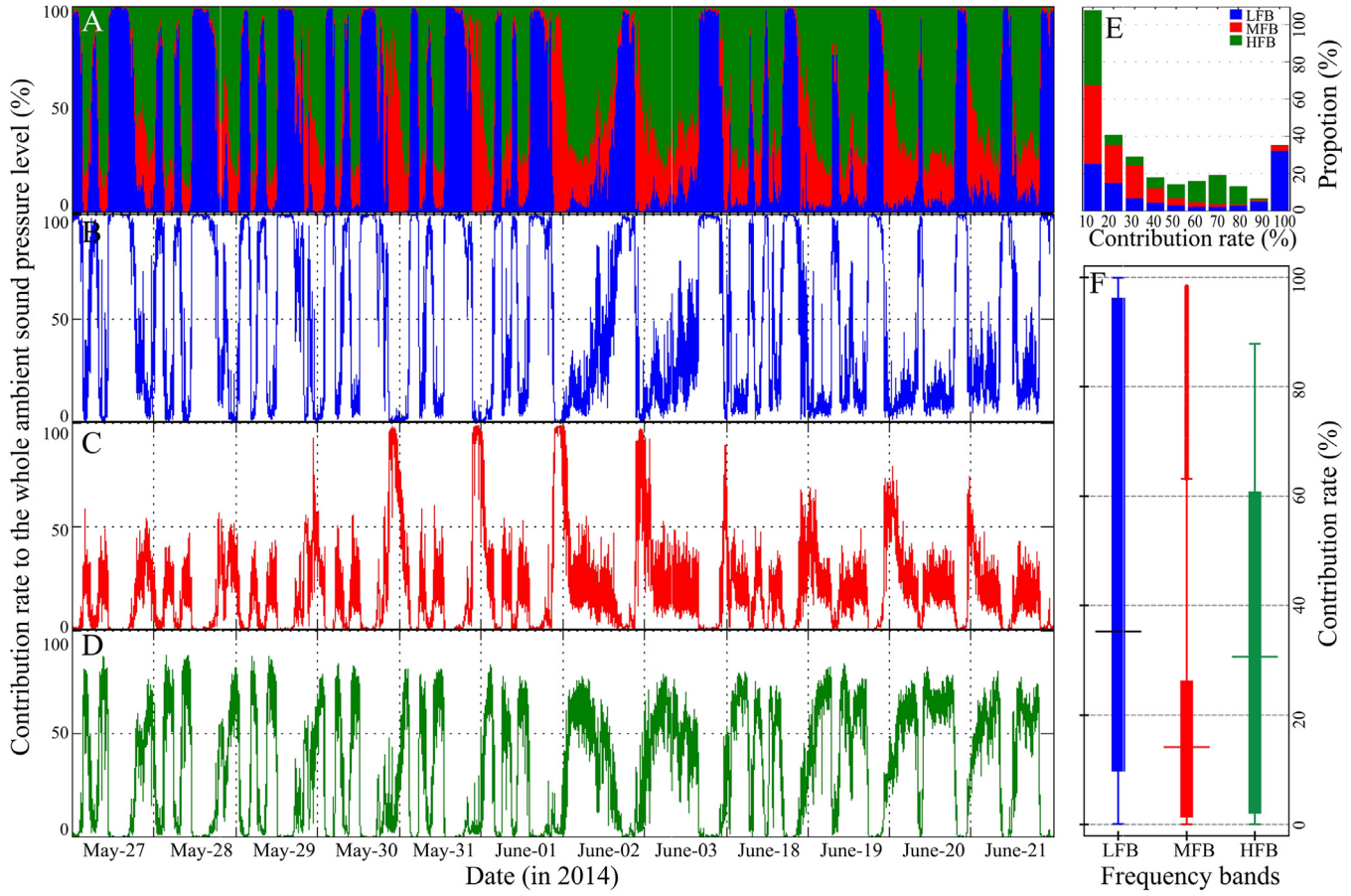

Fig. 10. Contributions of the three SPL bands to the overall ambient SPL. (A) Stacked bar plot showing the relative contribution rate of the three SPL bands with detailed information on SPL_{lfb} in B, SPL_{mfb} in C and SPL_{hfb} in D by time of day (X axis). The stacked bar plot in E shows the graded distribution pattern of the three bands with summarized contributions shown in the boxplot in F.

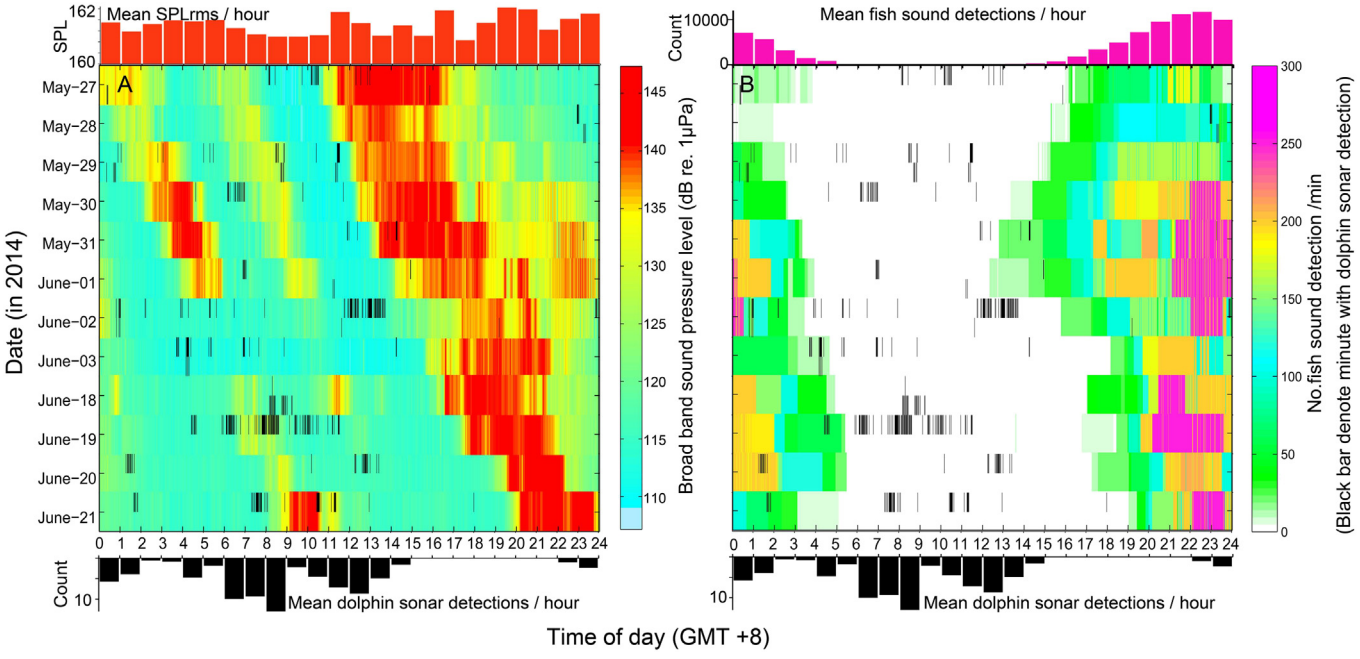

Fig. 11. Overlay of (A) broad band ambient sound pressure level and humpback dolphin sounds and (B) fish sounds and humpback dolphin sounds detection as a function of the time of day (X axis) and date (Y axis). Humpback dolphin whistles are denoted at the top half of each grid cell and dolphin click train is denoted along the bottom half of each grid cell. Averaged ambient broadband sound pressure levels (histograms above A), dolphin sonar (by combining dolphin whistles with click trains, histograms below A and B) and fish sounds (histograms above B) detected in each per hour of the monitoring periods are also given.

Table 1
Results of a two-way ANOVA (diel × tidal) of broadband SPL_{rms} and three subdivided frequency bands of the Pearl River Estuary. The main effects of diel and tidal and interactive effects of diel × tidal were identified as significant sources of variability at the three band sound pressure levels. Bold numbers indicate significant effects ($p < 0.01$).

Source	Dependent variable	Type III sum of squares	df	Mean square	F	Sig.
Corrected model	SPL_{rms}	2.964	19	0.156	335.139	**0.000**
	SPL_{lfb}	0.021	19	0.001	258.202	**0.000**
	SPL_{mfb}	0.000	19	1.820E-5	427.088	**0.000**
	SPL_{hfb}	1.121E-6	19	5.900E-8	752.067	**0.000**
Intercept	SPL_{rms}	1.921	1	1.921	4.126E3	**0.000**
	SPL_{lfb}	0.004	1	0.004	997.256	**0.000**
	SPL_{mfb}	1.753E-5	1	1.753E-5	411.324	**0.000**
	SPL_{hfb}	1.766E-6	1	1.766E-6	2.251E4	**0.000**
Diel	SPL_{rms}	0.733	4	0.183	393.403	**0.000**
	SPL_{lfb}	0.004	4	0.001	218.916	**0.000**
	SPL_{mfb}	0.000	4	3.455E-5	810.602	**0.000**
	SPL_{hfb}	7.392E-7	4	1.848E-7	2.356E3	**0.000**
Tidal	SPL_{rms}	0.612	3	0.204	438.261	**0.000**
	SPL_{lfb}	0.005	3	0.002	369.693	**0.000**
	SPL_{mfb}	1.263E-5	3	4.209E-6	98.758	**0.000**
	SPL_{hfb}	5.458E-8	3	1.819E-8	231.895	**0.000**
Diel × tidal	SPL_{rms}	0.463	12	0.039	82.827	**0.000**
	SPL_{lfb}	0.005	12	0.000	101.560	**0.000**
	SPL_{mfb}	0.000	12	1.459E-5	342.334	**0.000**
	SPL_{hfb}	1.331E-7	12	1.109E-8	141.366	**0.000**
Error	SPL_{rms}	9.305	19,987	0.000		
	SPL_{lfb}	0.086	19,987	4.298E-6		
	SPL_{mfb}	0.001	19,987	4.262E-8		
	SPL_{hfb}	1.568E-6	19,987	7.845E-11		
Total	SPL_{rms}	20.130	20,007			
	SPL_{lfb}	0.128	20,007			
	SPL_{mfb}	0.001	20,007			
	SPL_{hfb}	7.623E-6	20,007			
Corrected total	SPL_{rms}	12.269	20,006			
	SPL_{lfb}	0.107	20,006			
	SPL_{mfb}	0.001	20,006			
	SPL_{hfb}	2.689E-6	20,006			

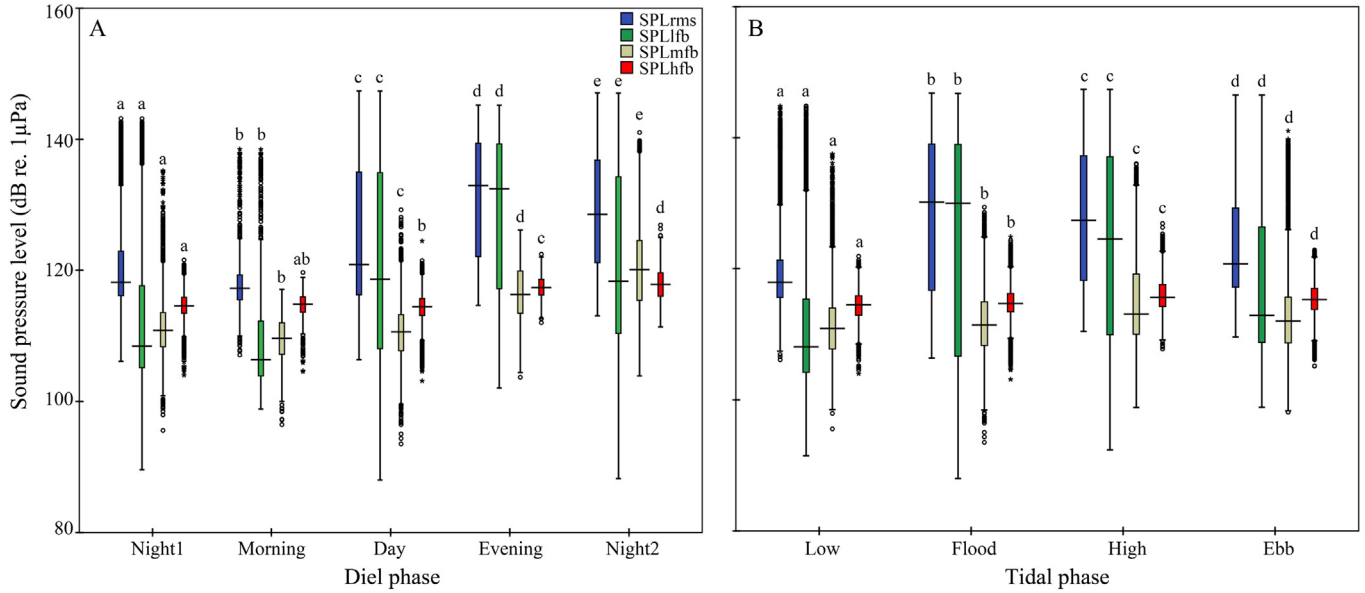

Fig. 12. Box plot of the broadband sound pressure levels and subdivided three frequency band (low frequency, middle frequency and high frequency) sound pressure levels as a function of diel (A) and tidal phases (B). The center of each box is the median value, the upper and lower box borders are the first quartile and the third quartile. The whiskers extend to extreme data within 1.5 times of the inter quartile range beyond the box borders. Outliers (open circles) are the data outside the whisker. Box with different lowercase letters refer to a Tamhane's T2 post-hoc multiple-comparison test that yielded significant results at $p < 0.05$.

(Hildebrand, 2009). Wind is capable of generating prominent levels of broadband noise (Wenz, 1962) and a strong relation between wind speed and ambient sound for frequencies above 500 Hz was observed in the Atlantic sector of the Southern Ocean (Menze et al., 2017). Shear currents can also induce strumming or flow noise (Menze et al., 2017) and even generate self-noise on a mooring system (Urick, 1983). In this study, the majority of temporal patterns of low frequency bands were characterized by three peak times per day (Figs. 6 and 9), which contradicts local semidiurnal tidal rhythms. Additionally, dynamic SPL_{rms} and SPL_{lfb} patterns did not occur in phase with local tidal conditions

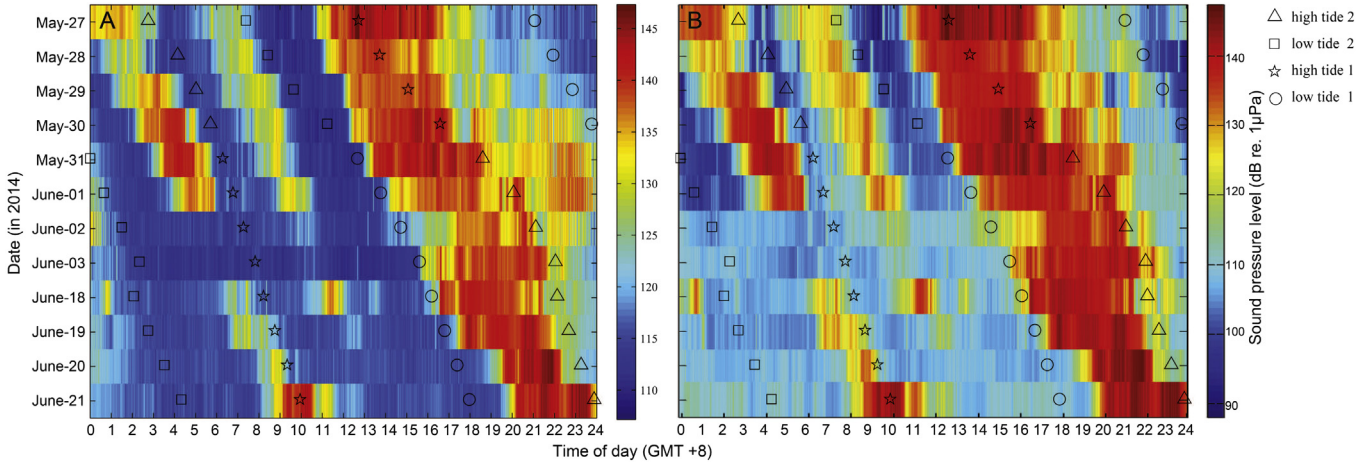

Fig. 13. Timing of tidal phases compared to the temporal patterns of (A) broadband sound pressure levels (SPL_{rms}) and SPL_{lfb} (B) as a function of the time of day (X axis) and date (Y axis). For semidiurnal tidal conditions, the peak tidal phase generally includes the first and secondary high tide periods. The valley tidal phase generally covers the first and secondary low tide period.

(Fig. 13), which precludes the hypothesis that the low frequency band noise observed in this study can be ascribed to self-noise in the mooring system caused by currents. Shipping activity may constitute another potential source. Source origins of the low frequency band noise observed in this study deserve further study.

Former study indicated that fish sounds obtained from the Pearl River Estuary tend to exhibit a pulse train structure with most energy levels falling below 4000 Hz (Wang et al., 2017). The peak frequency of fish sounds from the Pearl River Estuary ranges from 500 Hz to 2600 Hz (Wang et al., 2017), which covers much of the middle frequency band defined in this study (282 Hz–2238 Hz). Additionally, temporal patterns of fish sound detection rates correspond very well with those of SPL_{mfb} (Fig. S2), indicating that the middle frequency band defined in this study might be dominated and contributed to by soniferous fish.

Snapping shrimp (*Synalpheus parneomeris*) can produce very broad band impulsive signals, within a spectrum frequency range of 2 kHz to 200 kHz and are major sources of biological noise in temperate and tropical waters (Au and Banks, 1998). Snapping shrimp have also been observed to significantly change ambient sound levels in shallow temperate and tropical waters of the Tropical Eastern Pacific (Staaterman et al., 2013). In this study, SPL_{pk} was used to characterize the presence of impulsive sound, the majority of which is produced by snapping shrimp, indicating that they are a major source of biological noise in the research area. In addition to emitting high-frequency pulsed sounds for echolocation and navigation, humpback dolphins can produce frequency-modulated narrow-band whistles for communication purposes. The fundamental frequency of humpback dolphin whistles can reach 33,000 Hz (Wang et al., 2013) with apparent source levels of 137.4 dB re 1 μPa in rms (Wang et al., 2016). Snapping shrimp and marine mammal sounds may be the source of the high frequency band examined in this study.

In this study, the contributions to overall ambient SPL by SPL_{lfb}, SPL_{mfb} and SPL_{hfb} were measured as 35.24%, 14.14% and 30.61% (median), respectively. The low frequency band SPL was found to be the predominant signal source for the soundcape. The proportion of time with contributions of over 90% to the overall soundscape ascribed to SPL_{lfb} accounts for 32.3%, which is significantly higher than the value for SPL_{hfb} (0%). SPL_{mfb}, which was proposed to be caused by fish occasionally dominated the soundscape. Time contributions of > 50% and 90% to the overall soundscape were 8.2% and 2.9%, respectively. SPL_{hfb} was found to be relatively faint compared to other frequency bands. Its proportion of time with contribution rates of lower than 10% of the overall soundscape was measured as 42.3%, which is higher than values found for SPL_{hfb} (39.9%) and for SPL_{lfb} (25.3%) (Fig. 10).

4.4. Importance of this study

PAM studies using autonomous recording units have resulted in tremendously important findings with respect to monitoring protected areas and marine species and are important for assessing potential environmental impacts of anthropogenic noise sources (Haver et al., 2018).

The investigation of the soundscape of the Pearl River Estuary is critical in addressing relevant data gaps to better understand temporal patterns of local ocean noise while also contributing to the growing field of soundscape ecology by providing critical baseline data on our changing oceans. Baseline data for the soundscape examined in this study can facilitate the evaluation of impacts of Guishang windfarm infrastructure construction on local aquatic environments through comparison of baseline data to postconstruction and/or postmitigation effort data.

4.5. Future research

Relative to the peak amplitude time of the low frequency band, the peak amplitude time of the middle frequency band lagged behind (Fig. S1). Since fish sounds were proposed to be the source of the middle frequency band, the biological cause of this phenomenon, this may serve as a way in which local fish avoid noise and this deserves further study.

Future studies of the soundscape of the Pearl River Estuary based on multiple sites extending across larger spatial scales to examine spatial and temporal variations may provide interesting comparisons and may illustrate soundscape complexity to a greater degree while also greatly improving baseline knowledge on impacts of the construction and operation of windfarms on local acoustic environments and marine mammals. From existing and future changes in patterns of ocean noise and animal distributions we can facilitate conservation and further effective action for the conservation of vulnerable local humpback dolphins by identifying opportunities to protect important wildlife habitats and to adopt noise mitigation strategies.

5. Conclusion

Via passive acoustic monitoring, the baseline soundscape of a Chinese White dolphin hotspot prior to windfarm construction in the Pearl River Estuary, China was analyzed. The broad band root-mean-square sound pressure level (SPL_{rms}) measured every minute was recorded as 121.05 ± 8.44 dB (median ± QD) with a P5-P95 range of

113.44–141.62 dB. By cluster analysis, all 1/3 octave band power spectra can be grouped into three frequency bands, i.e., low frequency, middle frequency and high frequency bands with frequency ranges of 2.82–281, 282–2238 and 2239–44,686 Hz, respectively. Contribution rates to the overall ambient SPL value by SPL_{lfb}, SPL_{mfb} and SPL_{hfb} were measured as 35.24%, 14.14% and 30.61% (median), respectively. Significant variations were observed in SPL_{rms} values and the three band SPLs across different diel and tidal conditions with a GLM model. The frequency band and temporal pattern of the SPL of the middle frequency band correspond well with the frequency band and frequency of fish sound, showing that fish are the source of the middle frequency band. The baseline soundscape can shield some light for the evaluation of effects of an offshore windfarm on acoustic environments and aquatic animals by comparing the baseline to postconstruction data. Such risk assessments offer a way to prioritize areas in which mitigation is needed most for species vulnerable to current increases in anthropogenic noise. Our data can assist with the conservation of local vulnerable humpback dolphins by identifying important dolphin habitats and presenting standard soundscapes for noise management. Our results can thus help facilitate mitigation decisions and strategies of conservation and management.

Acknowledgements

Grants for this study were provided by the National Natural Science Foundation of China (NSFC, Grant No. 41806197) to Zhi-Tao Wang, the NSFC (Grant No. 31070347), the Chinese Ministry of Science and Technology of China (Grant No. 2011BAG07B05-3) to Ding Wang and the NSFC (Grant No. 31170501) to Ke-Xiong Wang. We also thank associate editor Paul Shin and the reviewers for their comments and suggestions, which improved the manuscript.

Competing interests

The authors have no competing interests to declare.

Appendix A. Supplementary data

Supplementary data to this article can be found online at https://doi.org/10.1016/j.marpolbul.2019.02.013.

References

Akamatsu, T., Matsuda, A., Suzuki, S., Wang, D., Wang, K.X., Suzuki, M., Muramoto, H., Sugiyama, N., Oota, K., 2005. New stereo acoustic data logger for free-ranging dolphins and porpoises. Mar. Technol. Soc. J. 39, 3–9.
Au, W.W.L., Banks, K., 1998. The acoustics of the snapping shrimp Synalpheus parneomeris in Kaneohe Bay. J. Acoust. Soc. Am. 103, 41–47.
Bailey, H., Senior, B., Simmons, D., Rusin, J., Picken, G., Thompson, P.M., 2010. Assessing underwater noise levels during pile-driving at an offshore windfarm and its potential effects on marine mammals. Mar. Pollut. Bull. 60, 888–897.
Banner, A., 1972. Use of sound in predation by young lemon sharks, Negaprion brevirostris (Poey). Bull. Mar. Sci. 22, 251–283.
Barros, N.B., 1993. Feeding Ecology and Foraging Strategies of Bottlenose Dolphins on the Central East Coast of Florida. University of Miami.
Barros, N.B., Myrberg, A.A., 1987. Prey detection by means of passive listening in bottlenose dolphins (Tursiops truncatus). J. Acoust. Soc. Am. 82, S65.
Barros, N.B., Jefferson, T.A., Parsons, E.C.M., 2004. Feeding habits of indo-Pacific humpback dolphins (Sousa chinensis) stranded in Hong Kong. Aquat. Mamm. 30, 179–188.
Chen, T., Hung, S.K., Qiu, Y.S., Jia, X.P., Jefferson, T.A., 2010. Distribution, abundance, and individual movements of Indo-Pacific humpback dolphins (Sousa chinensis) in the Pearl River Estuary, China. Mammalia 74, 117–125.
Cloern, J.E., Abreu, P.C., Carstensen, J., Chauvaud, L., Elmgren, R., Grall, J., Greening, H., Johansson, J.O.R., Kahru, M., Sherwood, E.T., Xu, J., Yin, K., 2016. Human activities and climate variability drive fast-paced change across the world's estuarine–coastal ecosystems. Glob. Chang. Biol. 22, 513–529.
Coquereau, L., Lossent, J., Grall, J., Chauvaud, L., 2017. Marine soundscape shaped by fishing activity. R. Soc. Open Sci. 4.
Dähne, M., Peschko, V., Gilles, A., Lucke, K., Adler, S., Ronnenberg, K., Siebert, U., 2014. Marine mammals and windfarms: effects of alpha ventus on harbour porpoises. In: Federal, M, Hydrographic, A, Federal Ministry for the Environment, N.C, Nuclear, S (Eds.), Ecological Research at the Offshore Windfarm Alpha Ventus: Challenges, Results and Perspectives. Springer Fachmedien Wiesbaden, Wiesbaden, pp. 133–149.
Ellison, W., Southall, B., Clark, C., Frankel, A., 2012. A new context-based approach to assess marine mammal behavioral responses to anthropogenic sounds. Conserv. Biol. 26, 21–28.
Fish, M.P., Mowbray, W.H., 1970. Sound of Western North Atlantic Fishes. The Johns Hopkins Press, Baltimore and London.
Fury, C.A., Harrison, P.L., 2011. Seasonal variation and tidal influences on estuarine use by bottlenose dolphins (Tursiops aduncus). Estuar. Coast. Shelf Sci. 93, 389–395.
Gannon, D.P., Barros, N.B., Nowacek, D.P., Read, A.J., Waples, D.M., Wells, R.S., 2005. Prey detection by bottlenose dolphins, Tursiops truncatus: an experimental test of the passive listening hypothesis. Anim. Behav. 69, 709–720.
Guan, S., Lin, T.-H., Chou, L.-S., Vignola, J., Judge, J., Turo, D., 2015. Dynamics of soundscape in a shallow water marine environment: a study of the habitat of the Indo-Pacific humpback dolphin. J. Acoust. Soc. Am. 137, 2939–2949.
Guilherme-Silveira, F., Silva, F., 2009. Diurnal and tidal pattern influencing the behaviour of Sotalia guianensis on the north-eastern coast of Brazil. Mar. Biodiv. Rec. 2, e122.
Haver, S.M., Gedamke, J., Hatch, L.T., Dziak, R.P., Van Parijs, S., McKenna, M.F., Barlow, J., Berchok, C., DiDonato, E., Hanson, B., Haxel, J., Holt, M., Lipski, D., Matsumoto, H., Meinig, C., Mellinger, D.K., Moore, S.E., Oleson, E.M., Soldevilla, M.S., Klinck, H., 2018. Monitoring long-term soundscape trends in U.S. Waters: the NOAA/NPS Ocean Noise Reference Station Network. Mar. Policy 90, 6–13.
Hildebrand, J.A., 2009. Anthropogenic and natural sources of ambient noise in the ocean. Mar. Ecol. Prog. Ser. 395, 5–20.
Jefferson, T.A., Smith, B.D., 2016. Re-assessment of the conservation status of the Indo-Pacific humpback dolphin (*Sousa chinensis*) using the IUCN red list criteria. In: Advances in Marine Biology. Academic Press, pp. 1–26.
Jefferson, T.A., Hung, S.K., Law, L., Torey, M., Tregenza, N., 2002. Distribution and abundance of finless porpoises in Hong Kong and adjacent waters of China. Raffles Bull. Zool. 50, 43–56.
Karczmarski, L., Huang, S.-L., Or, C.K.M., Gui, D., Chan, S.C.Y., Lin, W., Porter, L., Wong, W.-H., Zheng, R., Ho, Y.-W., Chui, S.Y.S., Tiongson, A.J.C., Mo, Y., Chang, W.-L., Kwok, J.H.W., Tang, R.W.K., Lee, A.T.L., Yiu, S.-W., Keith, M., Gailey, G., Wu, Y., 2016. Humpback dolphins in Hong Kong and the Pearl River Delta: status, threats and conservation challenges. In: Advances in Marine Biology. Academic Press, pp. 27–64.
Kitting, C.L., 1979. The use of feeding noises to determine the algal foods being consumed by individual intertidal molluscs. Oecologia 40, 1–17.
Luczkovich, J.J., Daniel, H.J., Hutchinson, M., Jenkins, T., Johnson, S.E., Pullinger, R.C., Sprague, M.W., 2000. Sounds of sex and death in the sea: bottlenose dolphin whistles suppress mating choruses of silver perch. Bioacoustics 10, 323–334.
Madsen, P.T., Wahlberg, M., Tougaard, J., Lucke, K., Tyack, P., 2006. Wind turbine underwater noise and marine mammals: implications of current knowledge and data needs. Mar. Ecol. Prog. Ser. 309, 279–295.
Menze, S., Zitterbart, D.P., van Opzeeland, I., Boebel, O., 2017. The influence of sea ice, wind speed and marine mammals on Southern Ocean ambient sound. R. Soc. Open Sci. 4.
Montgomery, J.C., Radford, C.A., 2017. Marine bioacoustics. Curr. Biol. 27, R502–R507.
Parra, G.J., Jedensjö, M., 2014. Stomach contents of Australian snubfin (Orcaella heinsohni) and indo-Pacific humpback dolphins (Sousa chinensis). Mar. Mamm. Sci. 30, 1184–1198.
Pijanowski, B., Farina, A., Gage, S., Dumyahn, S., Krause, B., 2011a. What is soundscape ecology? An introduction and overview of an emerging new science. Landsc. Ecol. 26, 1213–1232.
Pijanowski, B.C., Villanueva-Rivera, L.J., Dumyahn, S.L., Farina, A., Krause, B.L., Napoletano, B.M., Gage, S.H., Pieretti, N., 2011b. Soundscape ecology: the science of sound in the landscape. Bioscience 61, 203–216.
Preen, A., 2004. Distribution, abundance and conservation status of dugongs and dolphins in the southern and western Arabian Gulf. Biol. Conserv. 118, 205–218.
Radford, C., Stanley, J., Tindle, C., Montgomery, J., Jeffs, A., 2010. Localised coastal habitats have distinct underwater sound signatures. Mar. Ecol. Prog. Ser. 401, 21–29.
Ren, X.M., Gao, D.Z., Yao, Y.L., Yang, F., Liu, J.F., Xie, F.J., 2007. Occurrence and characteristic of sound in large yellow croaker (Pseudosciaena crocea). J. Dalian Fish. Univ. 22, 123–128 (in chinese with english abstract).
Richardson, W.J., Greene, C.R.J., Malme, C.I., Thompson, D.H., 1995. Marine Mammals and Noise. Academic Press San Diego.
Romesburg, C., 2004. Cluster Analysis for Researchers. Lulu Press, Raleigh, USA.
Seger, K.D., Thode, A.M., Swartz, S.L., Urbán, R.J., 2015. The ambient acoustic environment in Laguna San Ignacio, Baja California Sur, Mexico. J. Acoust. Soc. Am. 138, 3397–3410.
Simpson, S.D., Radford, A.N., Nedelec, S.L., Ferrari, M.C.O., Chivers, D.P., McCormick, M.I., Meekan, M.G., 2016. Anthropogenic noise increases fish mortality by predation. Nat. Commun. 7.
Slabbekoorn, H., Bouton, N., 2008. Soundscape orientation: a new field in need of sound investigation. Anim. Behav. 76, e5–e8.
Staaterman, E., Rice, A.N., Mann, D.A., Paris, C.B., 2013. Soundscapes from a Tropical Eastern Pacific reef and a Caribbean Sea reef. Coral Reefs 32, 553–557.
Staaterman, E., Paris, C.B., DeFerrari, H.A., Mann, D.A., Rice, A.N., D'Alessandro, E.K., 2014. Celestial patterns in marine soundscapes. Mar. Ecol. Prog. Ser. 508, 17–32.
Tavolga, W., Popper, A., Fay, R., 1981. Hearing and Sound Communication in Fishes. Springer-Verlag, New York, Berlin.
Thompson, P.M., Lusseau, D., Barton, T., Simmons, D., Rusin, J., Bailey, H., 2010. Assessing the responses of coastal cetaceans to the construction of offshore wind turbines. Mar. Pollut. Bull. 60, 1200–1208.
Todd, V.L.G., Pearse, W.D., Tregenza, N.C., Lepper, P.A., Todd, I.B., 2009. Diel echolocation activity of harbour porpoises (Phocoena phocoena) around North Sea offshore gas installations. ICES J. Mar. Sci. 66, 734–745.

Urick, R.J., 1983. Principles of Underwater Sound. McGraw-Hill, New York.
Wang, Z.-T., Fang, L., Shi, W.-J., Wang, K.-X., Wang, D., 2013. Whistle characteristics of free-ranging Indo-Pacific humpback dolphins (Sousa chinensis) in Sanniang Bay, China. J. Acoust. Soc. Am. 133, 2479–2489.
Wang, Z.-T., Akamatsu, T., Wang, K.-X., Wang, D., 2014a. The diel rhythms of biosonar behavior in the Yangtze finless porpoise (Neophocaena asiaeorientalis asiaeorientalis) in the port of the Yangtze river: the correlation between prey availability and boat traffic. PLoS One 9, e97907.
Wang, Z.-T., Wu, Y.-P., Duan, G.-Q., Cao, H.-J., Liu, J.-C., Wang, K.-X., Wang, D., 2014b. Assessing the underwater acoustics of the world's largest vibration hammer (OCTA-KONG) and its potential effects on the Indo-Pacific humpbacked dolphin (Sousa chinensis). PLoS One 9, e110590.
Wang, Z.-T., Akamatsu, T., Mei, Z.-G., Dong, L.-j., Imaizumi, T., Wang, K.-X., Wang, D., 2015a. Frequent and prolonged nocturnal occupation of port areas by Yangtze finless porpoises (Neophocaena asiaeorientalis): forced choice for feeding? Integr. Zool. 10, 122–132.
Wang, Z.-T., Nachtigall, P.E., Akamatsu, T., Wang, K.-X., Wu, Y.-P., Liu, J.-C., Duan, G.-Q., Cao, H.-J., Wang, D., 2015b. Passive acoustic monitoring the diel, lunar, seasonal and tidal patterns in the biosonar activity of the Indo-Pacific humpback dolphins (Sousa chinensis) in the Pearl River Estuary, China. PLoS One 10, e0141807.
Wang, Z.-T., Au, W., Rendell, L., Wang, K.-X., Wu, H.-P., Wu, Y.-P., Liu, J.-C., Duan, G.-Q., Cao, H.-J., Wang, D., 2016. Apparent source levels and active communication space of whistles of free-ranging Indo-Pacific humpback dolphins (Sousa chinensis) in the Pearl River Estuary and Beibu Gulf, China. PeerJ 4, e1695.
Wang, Z.-T., Nowacek, D.P., Akamatsu, T., Wang, K.-X., Liu, J.-C., Duan, G.-Q., Cao, H.-J., Wang, D., 2017. Diversity of fish sound types in the Pearl River Estuary, China. PeerJ 5, e3924.
Wenz, G.M., 1962. Acoustic ambient noise in the ocean: spectra and sources. J. Acoust. Soc. Am. 34, 1936–1956.
Whitehead, P.J.P., Blaxter, J.H.S., 1989. Swimbladder form in clupeoid fishes. Zool. J. Linnean Soc. 97, 299–372.
Zar, J.H., 1999. Biostatistical Analysis. Prentice-Hall, Upper Saddle River, NJ.